DALTON
FULL PAPER

Nucleophilic addition *via* metal–metal bond cleavage in an osmium–antimony cluster

Guizhu Chen and Weng Kee Leong *

Department of Chemistry, National University of Singapore, Kent Ridge, 119260, Singapore

The room-temperature reaction of a number of two-electron nucleophiles with the osmium–antimony cluster $[Os_3(\mu\text{-}H)(CO)_{10}(\mu\text{-}SbPh_2)]$ **1** gave adducts $[Os_3H(CO)_{10}(\mu\text{-}SbPh_2)L]$ **2** (L = PPh_3 **a**, $AsPh_3$ **b**, $SbPh_3$ **c** or CO **d**), in which the antimony-bridged Os–Os bond has been cleaved in order to accommodate the incoming ligand. X-Ray crystallographic studies on **2b** and **2c** confirmed that the ligands L occupied an equatorial site of the Os_3Sb framework, while NMR studies indicated that the clusters **2a**–**2c** existed as isomeric mixtures, which probably differ in the arrangements of the ligand L relative to the antimony vertex. The reaction leading to the formation of **2b**, which was carried out at elevated temperature, also led to decarbonylation to a substituted analogue of **1** in which the ligand L was on the unbridged osmium.

Main group–transition metal cluster compounds are of current interest as they are expected to show structural and reactivity patterns that may be quite unlike those of the homometallic main group or transition-metal clusters. This is the expectation, *a priori*, from the interplay between the differing properties of the elements. Over the years there has been a steady movement towards the view that the main group elements in many cluster compounds should be regarded as an integral part of the cluster core, and not as mere appendages (ligands).[1–3] One of the points of contention between these two views is at what point a main group fragment should be better regarded as a ligand or as a cluster vertex; this delineation often falls at the μ bonding mode, the moiety under investigation in this study.

As has been pointed out by Whitmire,[2] antimony-containing clusters are the least represented among the Group 15 elements. In the particular area of osmium–Group 15 clusters, for instance, there is a vast body of data available on phosphorus-containing osmium clusters but hardly any on antimony–osmium clusters. Almost all the antimony-containing osmium clusters reported merely have the antimony as a terminal ligand (typically $SbPh_3$); the crystal structure of only one antimony–osmium cluster with the antimony as other than a terminal ligand has been reported.[3] This state of affairs is probably the result of expectations that antimony-containing clusters will behave very similarly to the phosphorus analogues, although that is an unlikely prospect as the relatively larger number of studies carried out on arsenic–osmium clusters show that these very often do not behave like their phosphorus analogues.[4,5] We report here some of our initial studies in this area which point to the uniqueness of antimony–osmium cluster chemistry.

Results and Discussion

The cluster $[Os_3(\mu\text{-}H)(CO)_{10}(\mu\text{-}SbPh_2)]$ **1**[6] reacted slowly at room temperature with the Group 15 nucleophiles EPh_3 (E = Ph, As or Sb) to give the adducts $[Os_3H(CO)_{10}(\mu\text{-}SbPh_2)L]$ **2a**–**2c** in high yields. The profiles of the CO stretching vibrations were all similar, indicating similar structures. The ^1H NMR spectra of **2a**–**2c** showed two resonances at *ca.* δ −7.8 and −8.1 in the high field region, indicative of the presence of terminal OsH and of isomers; the ^1H NMR signal for terminal OsH is usually at lower field (*ca.* δ −10) than that of an edge-bridging OS(μ-H)Os (*ca.* δ −15 to −25).[7] The presence of isomers was also reflected in the $^{31}P\text{-}\{^1H\}$ NMR spectrum for **2a**, which also showed two resonances.

The molecular structure of one of these isomers has been confirmed in the case of compounds **2b** and **2c** by single crystal X-ray crystallographic studies; the ORTEP[8] diagram of the molecular structure of **2b** is given in Fig. 1. In the case of **2b**, the position of the metal hydride was also located directly from a low-angle difference map. The structures of **2b** and **2c** show that the osmium–osmium bond bridged by the antimony atom has been cleaved; the Os(1)···Os(2) distances are 4.266 and 4.248 Å in **2b** and **2c**, respectively. This indicates that **1** has undergone a novel nucleophilic addition reaction in which a metal–metal bond has been cleaved (Scheme 1); the nucleophile occupies an

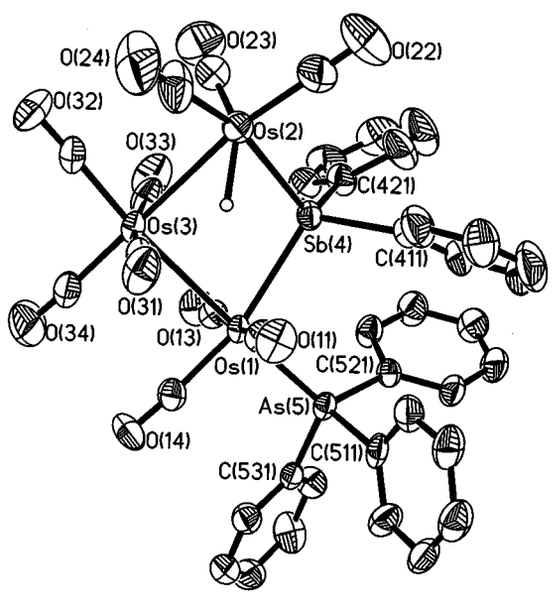

Fig. 1 An ORTEP diagram of compound **2b** (50% thermal ellipsoids)

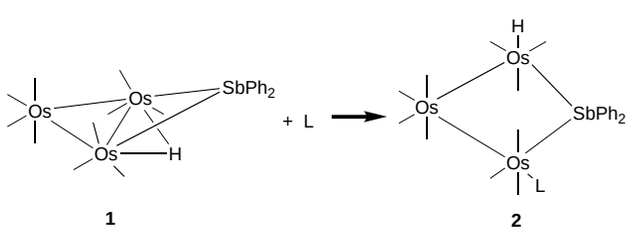

Scheme 1 Reaction of $[Os_3(\mu\text{-}H)(CO)_{10}(\mu\text{-}SbPh_2)]$ **1** with nucleophiles L [EPh_3 (E = P, As or Sb) or CO] to give $[Os_3H(CO)_{10}(\mu\text{-}SbPh_2)L]$ **2**

equatorial position on the Os_3Sb ring. To our knowledge, such a reaction mode has not been observed in the triosmium–phosphorus or –arsenic systems; two closely related examples from triosmium chemistry are the insertion of $SnCl_2$ into an Os–Os bond in $[Os_3(CO)_{11}(\mu\text{-}CH_2)]$ to form $[Os_3(CO)_{11}(\mu\text{-}CH_2)(\mu_3\text{-}SnCl_2)]$,[9] and the reaction of $[Os_3(CO)_{11}(MeCN)]$ with Me_2AsH to form $[Os_3H(CO)_{11}(\mu\text{-}AsMe_2)]$.[5] We have also verified that the phosphorus analogue of **1**, *viz* $[Os_3(\mu\text{-}H)(CO)_{10}(\mu\text{-}PPh_2)]$ did not react with PPh_3 at room temperature even after 1 week; at elevated temperatures it has been shown that orthometallation of one of the phenyl rings takes place and the orthometallated cluster could subsequently undergo nucleophilic attack with reversal of the orthometallation to give, for example, $[Os_3(\mu\text{-}H)(CO)_9(\mu\text{-}PPh_2)(PPh_2H)]$.[10] We believe that the reason for this difference in reactivity is due to the larger size of the antimony atom which disfavoured re-establishment of the cleaved Os–Os bond by ligand loss. This is also consistent with the observation that $[Os_3H(CO)_{11}(\mu\text{-}AsMe_2)]$ decarbonylated easily on silica gel,[5] while the clusters **2** were somewhat more stable.

As was mentioned above, the OsH resonances for compounds **2a**–**2c** consisted of two separate signals of unequal intensities, indicative of isomers. We believe that the two isomers in solution have structures differing in the orientation of the Group 15 ligand relative to the Sb atom. Consistent with this is the observation that the reaction of **1** with CO under ambient conditions gave the adduct $[Os_3H(CO)_{11}(\mu\text{-}SbPh_2)]$ **2d**, which showed only one resonance in the OsH region in its ^1H NMR spectrum. The IR spectrum of **2d** in the CO stretching region was similar to that[5] of the known $AsMe_2$ analogue [ν(CO) 2118w, 2078s, 2053m, 2047s, 2035vs, 2016m, 2011m, 1992m and 1977m cm^{-1}].

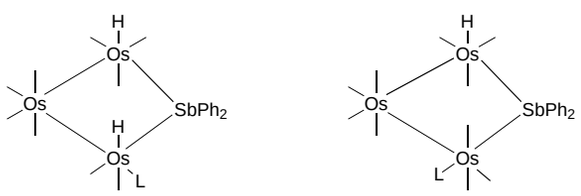

We have also found that a trace of a second product was sometimes obtained; this was formed in significant amounts at elevated temperatures. For example, the reaction of cluster **1** with $AsPh_3$ at 65 °C gave a 23% yield of a product with spectroscopic characteristics similar to those of the known clusters $[Os_3(\mu\text{-}H)(CO)_9(\mu\text{-}PPh_2)(PR_3)]$ [$PR_3 = PPh_2H$, $P(OMe)_3$ or $P(p\text{-}MeC_6H_4)_3$].[5] We have confirmed the identity of our product by a single crystal X-ray structural study (Fig. 2), and ^1H NMR evidence did not suggest the presence of any other isomers. The molecular structure of the product, $[Os_3(\mu\text{-}H)(CO)_9(\mu\text{-}SbPh_2)(AsPh_3)]$, **3b**, shows that the Os–Os bond has been re-established. Quite unexpectedly, the $AsPh_3$ occupies an equatorial position on the unique unbridged osmium.

There are at least three possible routes by which clusters **3** may be formed (Scheme 2). Path **a** involves direct decarbonylation of **1**. If this were indeed the reaction path then it must be the kinetic pathway since ambient-temperature reaction gave almost exclusively **2**. Furthermore, we have found **2** to be thermally fairly stable, indicating that any equilibrium between **1** and **2** lies largely towards the latter. Path **b** involves an orthometallation similar to that observed in $[Os_3(\mu\text{-}H)(CO)_{10}(\mu\text{-}PPh_2)]$;[10] we have found that heating **1** did not give any analogous product but a higher-nuclearity cluster.[11] The reaction of **2a** with an excess of PPh_3 led rapidly to the formation of **3a**; this observation, together with the thermal stability of **2a**, suggests the non-dissociative pathway **c**.

The structures of compounds **2b** and **2c** comprise a puckered Os_3Sb ring; the dihedral angles between the Os(1)Os(3)Os(2) and Os(1)Sb(4)Os(2) planes are 150.0 and 149.4°, respectively, compared to 112° in **1** or 108.1° in **3b**;[6] the only other reported example of this structural type in osmium–Group 15 cluster chemistry is that of $[Os_3H(CO)_{11}(\mu\text{-}AsMe_2)]$.[5] Interestingly, the Sb atoms are puckered away from, rather than towards, the OsH moiety. This must indicate an electronic origin for the puckering of the ring.

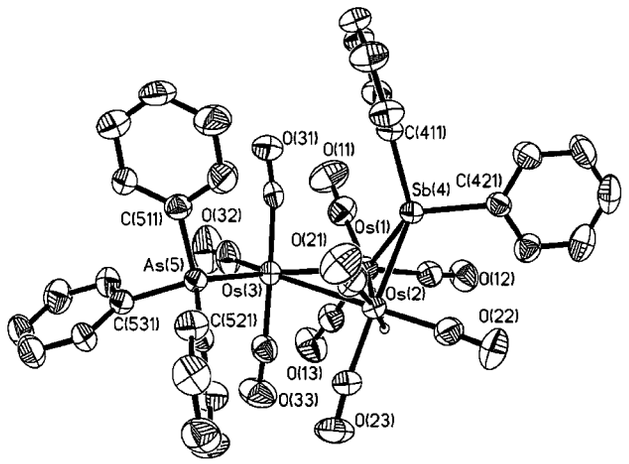

Fig. 2 An ORTEP diagram of compound **3b** (50% thermal ellipsoids). Os(1)–Os(2) 2.9973(3), Os(1)–Os(3) 2.8701(3), Os(2)–Os(3) 2.9423(3), Os(1)–Sb(4) 2.6433(4), Os(2)–Sb(4) 2.6253(4) and Os(3)–As(5) 2.4756(6) Å; Os(1)–Os(3)–Os(2) 62.070(8) and Os(1)–Sb(4)–Os(2) 69.346(12)°

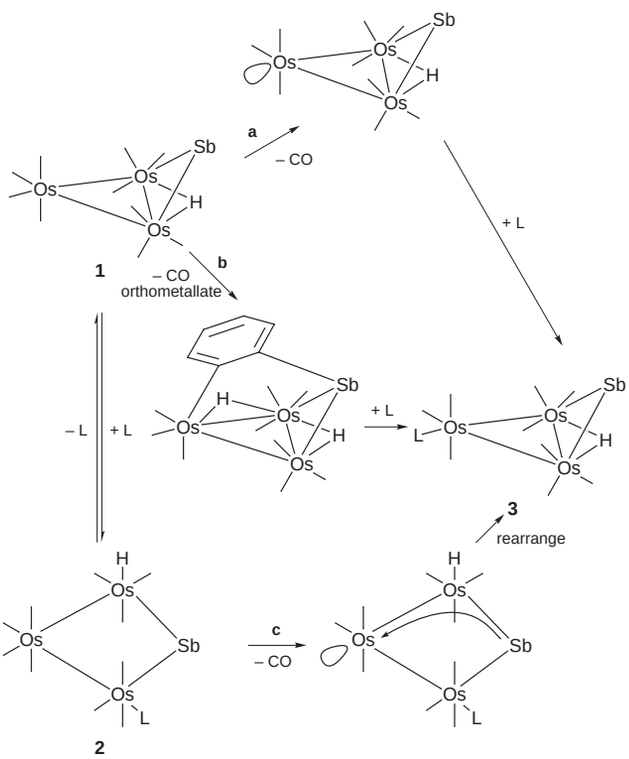

Scheme 2 Possible reaction pathways for the formation of compounds **3**

The increasingly stronger σ-donor ability in moving from $SbPh_3$ to $AsPh_3$ may be responsible for the shorter Os(1)–Sb(4) and Os(2)–Sb(4) lengths for compound **2c** as compared to **2b** (Table 1). Interestingly, the Os(1)–Sb(4)–Os(2) angles are similar for the two clusters, the differing lengths of the Os–Sb bonds being compensated by a change in the Os(1)···Os(2) distance instead. A more obvious consequence of the differing donor ability of $AsPh_3$ *vs.* $SbPh_3$ is the lengthening of the Os(1)–Os(3) bond [3.0137(5) and 2.9962(10) Å for **2b** and **2c**, respectively],

Table 1 Selected bond lengths (Å) and angles (°) for compounds **2b** and **2c**

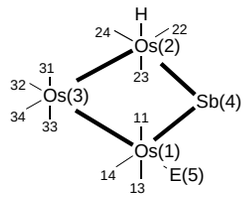

Bond parameter	**2b** (E = As)	**2c** (E = Sb)
Os(1) · · · Os(2)	4.266	4.248
Os(1)–Os(3)	3.0137(5)	2.9962(10)
Os(2)–Os(3)	2.9580(5)	2.9548(12)
Os(1)–Sb(4)	2.7191(6)	2.706(2)
Os(2)–Sb(4)	2.6441(7)	2.634(2)
Os(1)–E(5)	2.4918(9)	2.6238(13)
av. Os · · · C · · · O (axial) *	3.08	3.08
av. Os · · · C · · · O (equatorial) *	3.06	3.03
Os(1)–Sb(4)–Os(2)	105.37(2)	105.41(5)
Sb(4)–Os(1)–E(5)	100.45(2)	99.55(4)
Os(1)–Os(3)–Os(2)	91.171(13)	91.10(3)
Os(3)–Os(1)–Sb(4)	77.34(2)	77.39(3)
Os(3)–Os(2)–Sb(4)	79.48(2)	79.24(4)

* Average over [*d*(C–O) + *d*(Os–C)].

which is *trans* to the Group 15 ligand. Another structural consequence of electronic effects is the general observation that axial Os–CO bond lengths tend to be longer than equatorial ones. As has been argues elsewhere, a better way to gauge such an effect, given the inherent difficulty of locating light atoms in a heavy-atom structure with any precision, is to examine the Os · · · O distance rather than the Os–C bond length.[12] In **2b** and **2c**, therefore, it is found that the Os · · · O distances tend to be longer for axial (ranges of 3.067–3.12 and 3.06–3.10 Å, respectively, for **2b** and **2c**) than for equatorial carbonyls (ranges of 3.034–3.067 and 3.02–3.04 Å, respectively, for **2b** and **2c**); the upper limits for the equatorial carbonyls are for those *trans* to Sb(4). A very significant difference between **2b** and **2c** is the Sb(4)–Os(1)–E(5) bond angle [100.45(2) and 99.55(4)°, respectively]. This suggests that there is actually less steric repulsion between the EPh_3 and the $SbPh_2$ for E = Sb than for E = As, presumably because the phenyl rings, which are expected to be the main contributors to steric interaction between these two moieties, are further apart in **2c**; the Os(1)–E(5) lengths are 2.4918(9) and 2.6238(13) Å, respectively. It is tempting to ascribe the asymmetry between the Os(1)–Sb(4) and Os(2)–Sb(4) bond lengths to this steric interaction, but that this is also observed for $[Os_3H(CO)_{11}(\mu\text{-}AsMe_2)]$ [2.523(2) and 2.480(3) Å, respectively] which has a CO in place of EPh_3[5] suggests that this is not very likely. It may be argued that the reason is electronic, but we believe that the symmetry may be a consequence of the susceptibility of the Os–Sb and Os–As bonds to distortion, such as by crystal packing forces. In support of this we note that **3b** also shows the same asymmetry, despite the fact that the $AsPh_3$ ligand is now one bond further away; no such asymmetry is observed in $[Os_3(\mu\text{-}H)(CO)_9(\mu\text{-}PPh_2)\{P(OMe)_3\}]$.[10] Furthermore, the Os–As bond lengths in **2b** and **3b** are also very different [2.4918(9) and 2.4756(6) Å, respectively], indicating the wide range that such bond lengths can have.

Experimental

General procedures

All reactions and manipulations were carried out under nitrogen by using standard Schlenk techniques. Solvents were purified, dried, distilled, and stored under nitrogen prior to use. The NMR spectra were recorded on a Bruker ACF-300 FT-NMR spectrometer. Microanalyses were carried out by the microanalytical laboratory at the National University of Singapore. The starting material **1** was prepared by the published method;[6] all other reagents were from commercial sources and used as supplied.

Reactions of compound 1

With PPh_3. Cluster **1** (54 mg, 0.048 mmol) and an excess of PPh_3 (30 mg, 0.104 mmol) were stirred together in hexane (20 cm^3) at room temperature until the IR spectrum of the solution showed that the reactant had been consumed (≈2 d). Removal of the solvent followed by chromatographic separation on silica gel using dichloromethane–hexane (10 : 90, v/v) as eluent gave a trace amount of **3a**, followed by **2a** (54 mg, 81%) as yellow bands. Compound **2a** (Found: C, 35.85; H, 2.46. Calc. for $C_{40}H_{26}O_{10}Os_3PSb{\cdot}0.5C_6H_{14}$: C, 36.00; H, 2.30%): presence of hexane in crystals confirmed by ^1H NMR spectroscopy; $\tilde{\nu}_{max}/cm^{-1}$ (hexane) 2092m, 2058m, 2040w, 2017s, 1999m, 1980w (br) and 1968w (CO); ^1H NMR (300 MHz, [$^2H_8$]toluene, standard $SiMe_4$) δ 7.9–6.7 (m, Ph), −7.83 (s, OsH, major isomer) and −8.10 (s, OsH, minor isomer) (≈1 : 4 relative intensity); ^{31}P-{^1H} NMR ([$^2H_8$]toluene, standard 85% H_3PO_4) δ −5.56 (minor isomer) and −7.82 (major isomer). Compound **3a**: $\tilde{\nu}_{max}/cm^{-1}$ (hexane) 2071w, 2042s, 2022m, 1996vs, 1980m, 1972mw and 1954w (CO).

With $AsPh_3$. Cluster **1** (50 mg, 0.044 mmol) and an excess of $AsPh_3$ (40 mg, 0.13 mmol) were heated at 60 °C in hexane (20 cm^3). The reaction was monitored by IR spectroscopy until **1** had been consumed (≈9 h). Removal of the solvent followed by column chromatography with CH_2Cl_2–hexane (1 : 9, v/v) as eluent gave **3** (14.0 mg, 22.5%) and **2b** (39.5 mg, 62.2%) in that order. Compound **2b** (Found: C, 33.47; H, 2.05. Calc. for $C_{40}H_{26}AsO_{10}Os_3Sb$: C, 33.49; H, 1.81%): $\tilde{\nu}_{max}/cm^{-1}$ (hexane) 2093mw, 2054m, 2038mw, 2017s, 1998m, 1979mw (br) and 1968w (CO); ^1H NMR (300 MHz; [$^2H_8$]toluene, standard $SiMe_4$) δ 7.4–6.8 (m, Ph), −7.81 (s, OsH, minor isomer) and −8.16 (s, OsH, major isomer) (≈1 : 2 relative intensity). Compound **3b** (Found: C, 33.45; H, 1.90. Calc. for $C_{39}H_{26}AsO_9Os_3Sb$: C, 33.32; H, 1.85%); $\tilde{\nu}_{max}/cm^{-1}$ (hexane) 2072w, 2043s, 2020m, 1995s, 1978s, 1964w and 1953w; ^1H NMR (300 MHz, [$^2H_8$]toluene, standard $SiMe_4$) 7.5–7.0 (m, Ph) and −19.46 (s, OsHOs).

With $SbPh_3$. The reaction of cluster **1** (30 mg, 0.027 mmol) with $SbPh_3$ (30 mg, 0.085 mmol) was carried out in a similar manner to that for PPh_3 above. A similar work-up gave **2c** (35 mg, 89%) (Found: C, 32.79; H, 2.00. Calc. for $C_{40}H_{26}O_{10}Os_3Sb_2$: C, 32.40; H, 1.76%). $\tilde{\nu}_{max}/cm^{-1}$ (hexane) 2089w, 2053m, 2037mw, 2017s, 1998mw, 1978m (br) and 1967w (CO). ^1H NMR (300 MHz, solvent [$^2H_8$]toluene, standard $SiMe_4$) δ 7.9–6.8 (m, Ph), −7.88 (s, OsH, major isomer) and −8.15 (s, OsH, minor isomer) (≈3 : 2 relative intensity).

With CO. A hexane (20 cm^3) solution of cluster **1** (42 mg, 0.037 mmol) was placed in a Carius tube under CO (1 atm, 101 325 Pa) and heated in an oil-bath at 60 °C until the CO absorption bands of **1** in the IR spectrum had disappeared (≈9 h). Removal of the solvent followed by column chromatographic separation gave **2d** (34 mg, 79%) as an oil: $\tilde{\nu}_{max}/cm^{-1}$ (hexane) 2116w, 2077s, 2052mw, 2043m, 2035vs, 2015m, 1994mw and 1978mw (CO); ^1H NMR (300 MHz, [$^2H_8$]toluene, standard $SiMe_4$) δ 7.8–6.9 (m, Ph) and −8.45 (s, OsH).

Reaction of compound 2a with PPh_3

A solution of cluster **2a** (35 mg, 0.025 mmol) and an excess of PPh_3 (14 mg) in toluene (10 cm^3) was heated at 75 °C for 5 h. The solution changed from light yellow to orange. Chromatographic separation of the solution gave **3a** as the major band, identified spectroscopically.

Table 2 Crystal data $[Os_3H(CO)_{10}(\mu\text{-}SbPh_2)(AsPh_3)]$ **2b**, $[Os_3H(CO)_{10}(\mu\text{-}SbPh_2)(SbPh_3)]$ **2c** and $[Os_3(\mu\text{-}H)(CO)_9(\mu\text{-}SbPh_2)(AsPh_3)]$ **3b**

	2b	**2c**	**3b**
Empirical formula	$C_{40}H_{26}AsO_{10}Os_3Sb$	$C_{40}H_{26}O_{10}Os_3Sb_2$	$C_{39}H_{26}AsO_9Os_3Sb{\cdot}CH_2Cl_2$
Formula weight	1433.88	1480.71	1490.79
Crystal system	Triclinic	Triclinic	Monoclinic
Space group	$P\bar{1}$	$P\bar{1}$	$P2_1/c$
a/Å	12.5027(1)	12.7738(1)	12.8364(1)
b/Å	13.5169(2)	13.7256(3)	23.4741(2)
c/Å	14.6903(2)	14.6834(3)	14.6154(2)
α/°	63.659(1)	63.210(1)	—
β/°	89.945(1)	89.741(1)	101.127(1)
γ/°	80.756(1)	79.099(1)	—
U/Å^3	2169.13(5)	2247.03(7)	4321.17(8)
Z	2	2	4
μ/mm^{-1}	10.183	9.688	10.346
Reflections collected	18271	17678	33057
Independent reflections (R_{int})	10 423 (0.0421)	9401 (0.0636)	9974 (0.0378)
Final R [$I > 2\sigma(I)$]	0.0438	0.0688	0.0337
$wR2$ (all data)	0.1300	0.1948	0.0767

Crystallography

Crystals were grown from dichloromethane–hexane solutions and mounted on quartz fibres. X-Ray data were collected on a Siemens SMART CCD system, using Mo-Kα radiation, at ambient temperature [295(2) K]. Data were corrected for Lorentz-polarisation effects with the SMART suite of programs,[13] and for absorption effects with SADABS.[14] The final unit-cell parameters were obtained by least squares on 8192 (5174 for **2c**) strong reflections. Structural solution and refinement were carried out with the SHELXTL suite of programs.[15]

The structures were solved by direct methods to locate the heavy atoms, followed by difference maps for the light, non-hydrogen atoms. Phenyl H atoms were placed in calculated positions and given isotropic thermal parameters 1.5 times those of the C atoms to which they are attached. The metal hydride positions in compounds **2b** and **3b** were located by a low angle ($2\theta \leqslant 30°$) difference map. For **2c** the metal hydride was placed at 1.60 Å from Os(2) and *trans* to CO(23); an isotropic thermal parameter of 0.08 Å^2 was assigned. All non-hydrogen atoms were given anisotropic thermal parameters in the final model.

A disordered dichloromethane solvent molecule was found in structure **3b**. This was modelled with four alternative positions, with the occupancies summing to unity. The C–Cl bond lengths for the main site were restrained to be equal; those for the other sites were restrained to equal these. The C and Cl atoms were given a common isotropic thermal parameter for each atom type. Crystal data for all these compounds are given in Table 2.

CCDC reference number 186/1029.

Acknowledgements

This work was supported by the National University of Singapore (Research Grant No. RP 960677) and one of us (G. C.) thanks the University for a Research Scholarship.

References

1 For example, T. P. Fehlner, *Inorganometallic Chemistry*, Plenum, New York, 1992; W. A. Herrmann, *Angew. Chem.*, *Int. Ed. Engl.*, 1986, **25**, 56; J. N. Nicholls, *Polyhedron*, 1984, **3**, 1307.
2 K. H. Whitmire, *Adv. Organomet. Chem.*, 1998, **42**, 1.
3 W. K. Leong, *Bull. Sing. N. I. C.*, 1996, **24**, 51.
4 For example, K. Guldner, B. F. G. Johnson, J. Lewis, A. D. Massey and S. Bott, *J. Organomet. Chem.*, 1991, **408**, C13; K. Guldner, B. F. G. Johnson and J. Lewis, *J. Organomet. Chem.*, 1988, **355**, 419; A. J. Deeming, R. E. Kimber and M. Underhill, *J. Chem. Soc.*, *Dalton. Trans.*, 1973, 2589.
5 K. Guldner, B. F. G. Johnson, J. Lewis, S. M. Owen and P. R. Raithby, *J. Organomet. Chem.*, 1988, **341**, C45.
6 B. F. G. Johnson, J. Lewis, A. J. Whitton and S. G. Bott, *J. Organomet. Chem.*, 1990, **389**, 129.
7 For example, J. B. Keister and J. R. Shapley, *Inorg. Chem.*, 1982, **21**, 3304; W. Ehrenreich, M. Heberhold, G. Hermann, G. Suess-Fink, A. Gieren and T. Huebner, *J. Organomet. Chem.*, 1985, **294**, 183; S. C. Brown and J. Evans, *J. Chem. Soc.*, *Dalton. Trans.*, 1982, 1049; E. A. V. Ebsworth, A. P. McIntosh and M. Schroder, *J. Organomet. Chem.*, 1986, **312**, C41; F. W. B. Einstein, R. K. Pomeroy and A. C. Willis, *J. Organomet. Chem.*, 1986, **311**, 257.
8 C. K. Johnson, ORTEP, Report ORNL-5138, Oak Ridge National Laboratory, Oak Ridge, TN, 1976.
9 N. Viswanathan, E. D. Morrison, G. L. Geoffroy, S. J. Geib and A. L. Rheingold, *Inorg. Chem.*, 1986, **25**, 3100.
10 S. B. Colbran, P. T. Irele, B. F. G. Johnson, F. J. Lahoz, J. Lewis and P. R. Raithby, *J. Chem. Soc.*, *Dalton. Trans.*, 1989, 2023.
11 W. K. Leong and G. Chen, unpublished work.
12 W. K. Leong, F. W. B. Einstein and R. K. Pomeroy, *J. Cluster Sci.*, 1996, **7**, 121.
13 SMART, version 4.05, Siemens Energy & Automation Inc., Madison, WI, 1995.
14 G. M. Sheldrick, SADABS, University of Göttingen, 1996.
15 SHELXTL, version 5.03, Siemens Energy & Automation Inc., Madison, WI, 1995.

Received 28*th April* 1998; *Paper* 8/03169J